The Plant Cell, Vol. 24: 2963–2978, July 2012, www.plantcell.org

Functional Analyses of the Plant Photosystem I–Light-Harvesting Complex II Supercomplex Reveal That Light-Harvesting Complex II Loosely Bound to Photosystem II Is a Very Efficient Antenna for Photosystem I in State II[W]

Pierre Galka,[a,b,c,d] Stefano Santabarbara,[e,f] Thi Thu Huong Khuong,[a,b,c] Hervé Degand,[d] Pierre Morsomme,[d] Robert C. Jennings,[e,f] Egbert J. Boekema,[g] and Stefano Caffarri[a,b,c,1]

[a] Aix Marseille Université, Biologie Végétale et Microbiologie Environnementales, Laboratoire de Génétique et Biophysique des Plantes, 13288 Marseille, France

[b] Commissariat à l'Energie Atomique, Direction des Sciences du Vivant, Institut de Biologie Environnementale et Biotechnologie, 13288 Marseille, France

[c] Centre National de la Recherche Scientifique, Unité Mixte de Recherche 7265 Biologie Végétale et Microbiologie Environnementales, 13288 Marseille, France

[d] Institut des Sciences de la Vie, Université Catholique de Louvain, 1348 Louvain-la-Neuve, Belgium

[e] Consiglio Nazionale delle Ricerche, Istituto di Biofisica, 20133 Milan, Italy

[f] Dipartimento di Biologia, Università degli Studi di Milano, 20133 Milan, Italy

[g] Groningen University, Department of Biophysical Chemistry, Groningen Biomolecular Sciences and Biotechnology Institute, 9747 AG Groningen, The Netherlands

State transitions are an important photosynthetic short-term response that allows energy distribution balancing between photosystems I (PSI) and II (PSII). In plants when PSII is preferentially excited compared with PSI (State II), part of the major light-harvesting complex LHCII migrates to PSI to form a PSI-LHCII supercomplex. So far, little is known about this complex, mainly due to purification problems. Here, a stable PSI-LHCII supercomplex is purified from *Arabidopsis thaliana* and maize (*Zea mays*) plants. It is demonstrated that LHCIIs loosely bound to PSII in State I are the trimers mainly involved in state transitions and become strongly bound to PSI in State II. Specific Lhcb1-3 isoforms are differently represented in the mobile LHCII compared with S and M trimers. Fluorescence analyses indicate that excitation energy migration from mobile LHCII to PSI is rapid and efficient, and the quantum yield of photochemical conversion of PSI-LHCII is substantially unaffected with respect to PSI, despite a sizable increase of the antenna size. An updated PSI-LHCII structural model suggests that the low-energy chlorophylls 611 and 612 in LHCII interact with the chlorophyll 11145 at the interface of PSI. In contrast with the common opinion, we suggest that the mobile pool of LHCII may be considered an intimate part of the PSI antenna system that is displaced to PSII in State I.

INTRODUCTION

Oxygenic photosynthesis is driven by two photosystems (PSII and PSI) that work in series to convert light energy into chemical energy. A large part of the light is absorbed by the outer light-harvesting complexes (Lhcs), which contain most of the chlorophyll and carotenoid pigments and are peripherally associated with the PSs. For optimal linear electron transport, the light absorption of the two PSs needs to be balanced. PSI and PSII have different absorption spectra, and since the light quality and intensity can vary during the day, plants need to rapidly adjust the relative absorption cross sections of the two PSs. This regulation is based on the phenomenon called state transitions, which encompasses the relocation of Lhcs between PSII and PSI to adjust their relative antenna size (Allen, 1992; Wollman, 2001; Lemeille and Rochaix, 2010; Minagawa, 2011). In plants, light-harvesting complex II (LHCII) (the major light-harvesting antenna of PSII) is bound to PSII in State I, while in the State II condition, induced by preferential excitation of PSII, part of the LHCII pool is transferred to PSI. LHCII is a trimeric complex composed of a combination of three highly homologous Lhcb isoforms, Lhcb1-3, encoded by a large multigene family (Jansson, 1999).

State transitions are regulated by the reversible phosphorylation of Lhcb1 and Lhcb2 (Allen, 1992). Key proteins involved in sensing and activation of this phosphorylation have been recently discovered. The thylakoid proteins Stn7/Stt7 (Bellafiore et al., 2005; Lemeille et al., 2009) have been identified as kinases necessary to induce State I–to–State II transition in plants and algae, respectively. This kinase is activated by a redox signal linked to the reduction state of the plastoquinone pool under preferential PSII excitation and phosphorylates an N-terminal

[1] Address correspondence to stefano.caffarri@univ-amu.fr.
The author responsible for distribution of materials integral to the findings presented in this article in accordance with the policy described in the Instructions for Authors (www.plantcell.org) is: Stefano Caffarri (stefano.caffarri@univ-amu.fr).
[W] Online version contains Web-only data.
www.plantcell.org/cgi/doi/10.1105/tpc.112.100339

Thr on Lhcb1-2, a step considered indispensable to relocate it to PSI (Allen, 1992). On the contrary, under preferential PSI excitation or under dark-adapted conditions, a thylakoid peripheral protein (TAP38/PPH1) (Pribil et al., 2010; Shapiguzov et al., 2010) dephosphorylates LHCII upon which it returns to PSII.

Three different types of LHCII trimers can be distinguished, named S, M, and L, based on their strong (S), moderate (M), and loose (L) association with the PSII complex. The positions of the S and M trimers are well defined in the supercomplex (Dekker and Boekema, 2005), while the locations of loosely bound trimers are still debated. Under normal growth conditions, up to four LHCII trimers per monomeric PSII complex are found in the thylakoids (Peter and Thornber, 1991), meaning that two loosely bound trimers are in some way associated with PSII in the native membranes. The position of one L trimer has been suggested for PSII from spinach (*Spinacia oleracea*) (Boekema et al., 1999a), but this position is only occasionally occupied, and bound L trimers have not been observed in PSII from *Arabidopsis thaliana*.

So far, the identities of the LHCII trimers (S, M, or L) and of the specific Lhcb isoforms involved in state transitions have been controversial. It was shown that the Lhcb3 isoform is absent in stroma membranes under State II conditions (Bassi et al., 1988), suggesting that trimer M, which is particularly enriched in this subunit (Bassi and Dainese, 1992; Hankamer et al., 1997; Caffarri et al., 2004), is not involved in state transitions. However, more recent results suggest that trimer M is involved instead (Kouril et al., 2005; Damkjaer et al., 2009) and that Lhcb3 plays a role in modulating the rate of state transitions (Damkjaer et al., 2009).

The physiological importance of state transitions has been demonstrated clearly under fluctuating light conditions (Bellafiore et al., 2005; Tikkanen et al., 2010), indicating that it is a buffering system for dynamic low-light acclimation (Tikkanen et al., 2006). The physiological importance of state transitions in plants has been well documented also in seed production experiments (Frenkel et al., 2007; Wagner et al., 2008), which indicates a direct selective advantage for survival of the species. Another proof of its importance is its widespread presence in green photosynthetic organisms, including green algae such as *Chlamydomonas reinhardtii*, which diverged from the plant clade ~1000 million years ago (Bowman et al., 2007). However, in *C. reinhardtii*, state transitions are much more pronounced than in plants: A large reorganization of PSII outer antenna that also involves the displacement of the minor PSII antenna proteins CP29 and CP26 together with LHCII has been observed (Kargul et al., 2005; Takahashi et al., 2006; Iwai et al., 2008), indicating that the functional comparability between plants and *C. reinhardtii* is limited to some degree. Very recent results suggest that some PSII reorganization happens also in plants, and this would be an entry mechanism for state transitions (Dietzel et al., 2011).

Although many recent studies investigated the role of regulatory proteins involved in state transitions, the biochemical and spectroscopic properties of the plant PSI-LHCII complex formed in State II are yet to be characterized. Analysis of various PSI subunit mutants has suggested the importance of specific proteins for the docking of LHCII. In particular, mutants with impaired expression of PsaH show a strong reduction of state transitions (Lunde et al., 2000). Other subunits, such as PsaL and PsaO (and probably PsaP) are also important, likely participating in the formation of the domain involved in the interaction with LHCII (Jensen et al., 2004, 2007; Zhang and Scheller, 2004). The supercomplex PSI-LHCII formed in State II conditions has been visualized in an electron microscopy (EM) study on a heterogeneous preparation of solubilized thylakoids, and the electron density map indicated that one LHCII trimer is associated with the PSI core near the PsaA, -H, -L, and -K subunits (Kouril et al., 2005).

The purification of the supercomplex has been hampered by its instability in the presence of common detergents used for membrane protein purification, and only recently a direct investigation of some biochemical/spectroscopic properties has been performed on this supercomplex (Qin et al., 2011).

In this study, we improved a protocol for the isolation of pure and stable plant PSI-LHCII supercomplexes. These complexes have been studied by biochemical and spectroscopic methods to obtain information on the structure and functioning of the complex, in particular the excitation energy transfer (EET) process and the identity and composition of the LHCII trimer involved. We demonstrated that the trimers mainly involved in state transitions are a specific subset of LHCII, the LHCII loosely bound to PSII. Binding of the mobile trimer to PSI in State II is stable and stronger than binding of the same trimer to PSII in State I, and EET from the mobile LHCII to PSI is faster and more efficient than EET from the same trimers to PSII in State I.

RESULTS

Purification of the PSI-LHCII Supercomplex

To obtain the PSI-LHCII supercomplexes, the protocol of Zhang and Scheller (2004) based on thylakoid solubilization with digitonin, which was also shown to keep PSI-LHCII intact in native gels (Pribil et al., 2010), was modified to improve PSI-LHCII stability and purity. Stacked thylakoids in State II conditions were mildly solubilized with a digitonin/*n*-dodecyl-α-D-maltoside (α-DM) (1:0.2) mixture and fractionated by Suc gradient ultracentrifugation in the presence of 0.02% digitonin (Figure 1A, gradient 1). Using these conditions, stroma lamellae were solubilized, while most of the PSII-containing grana membranes remained unsolubilized, allowing the purification of PSI supercomplexes with negligible contamination by PSII. A second gradient was useful to improve the separation between PSI and PSI-LHCII supercomplexes (Figure 1A, gradient 2). The absorption spectrum of the PSI-LHCII complex showed a clear chlorophyll *b* enrichment compared with that of the PSI complex, as expected considering the high chlorophyll *b* content of LHCII (Figure 1B). The protein composition of the two fractions was analyzed by SDS-PAGE (Figure 1C), demonstrating the absence of LHCII in the PSI fractions as well as a strong enrichment of LHCII in the PSI-LHCII fraction.

We observed as an average of many different solubilizations that the PSI and PSI-LHCII band showed similar intensities. Thus, considering that some PSI-LHCII could be disrupted during preparation, we estimate that in our State II conditions at least 50% of PSI binds LHCII.

No other band containing supercomplexes of PSI and LHCII was detected in gradients of State II solubilized thylakoids

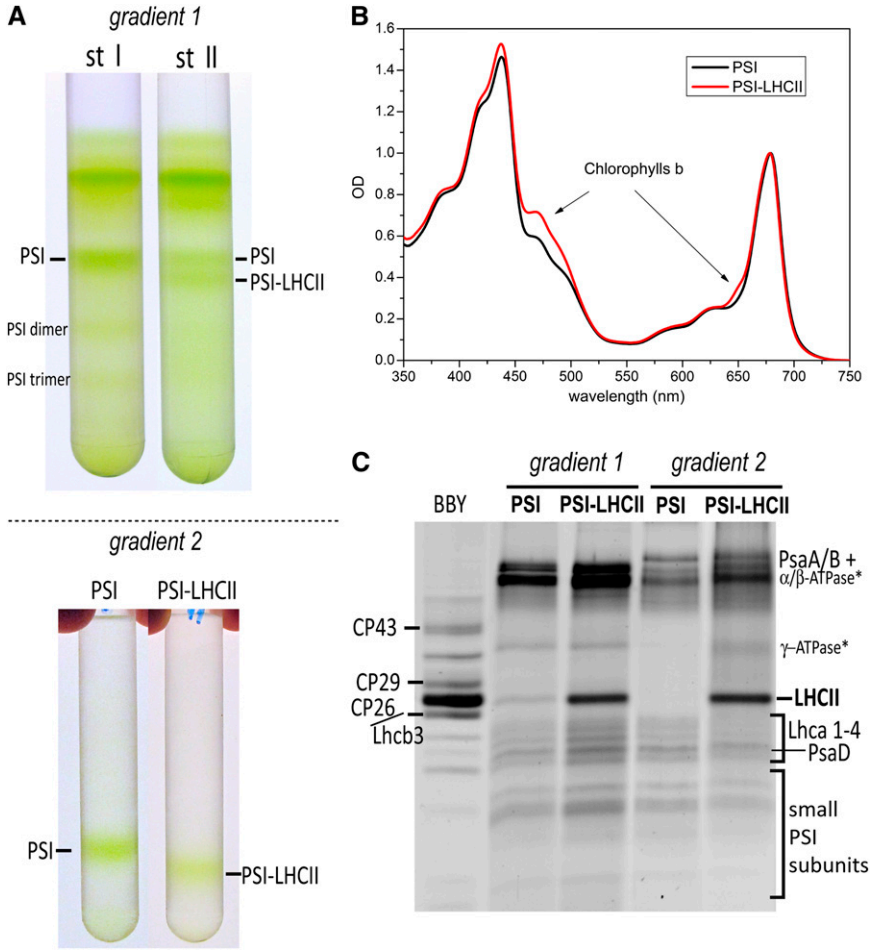

Figure 1. PSI-LHCII Purification, Absorption, and Protein Content.

(A) Suc gradient fractionation of solubilized *Arabidopsis* thylakoids in State I (st I) and State II (st II) conditions. State II thylakoids show an additional band below PSI, corresponding to the PSI-LHCII supercomplex. Bands corresponding to PSI and PSI-LHCII were harvested and further purified on a second gradient. Before gradient 2, PSI was treated with 0.02% α-DM to remove comigrating complexes (this treatment has negligible effect on PSI; see Figure 7 and stability section). Note that dimers and trimers of PSI are visible in the gradient (especially from State I plants).
(B) Absorption spectra of PSI and PSI-LHCII preparations normalized to the maximum in the red region.
(C) Sypro-stained SDS-PAGE gel of PSI and PSI-LHCII preparations from gradients 1 and 2. Grana membranes (BBY) are also loaded in the same gel to show the absence of other PSII proteins in the PSI/PSI-LHCII preparations. Some contamination from comigrating ATPase (*, similarly to previous works; see Zhang and Scheller, 2004; Pribil et al., 2010), which has a molecular mass similar to those of PSI/PSI-LHCII, is visible in the PSI-LHCII lane: high molecular mass subunits (α and β) migrate in the upper part of the gel, partially superimposed with the PsaA-B subunits of PSI; the γ-subunit, which has a molecular mass of ~36 kD, is also visible. Since ATPase does not bind pigment, its presence has no influence on the spectroscopic/biochemical measurements performed in this work. More detailed information on the Suc gradient fractions and on protein shown in the gel are presented as Supplemental Figure 1 online.

(Figure 1), as well in green native gels. An extensive analysis is presented as Supplemental Figure 1 online together with further information about the content of Suc gradient fractions.

Pigment Content and Purity of the Preparation

Quantification of the LHCII content in the PSI-LHCII complex was not possible from the SDS-PAGE (Figure 1) due to the different binding of the stain to different proteins depending on the protein sequence and size. Therefore, to quantify the LHCII content and to analyze the possible contamination of the PSI-LHCII fraction with PSI, we compared the pigment compositions of PSI and PSI-LHCII preparation. The analysis indicated a clear decrease of the chlorophyll *a*/*b* ratio in the PSI-LHCII supercomplex (4.91 ± 0.24) compared with PSI (8.17 ± 0.09). Using the recent PSI structure from pea (*Pisum sativum*) (Amunts et al., 2010) that reveals 173 chlorophylls, one can assume that PSI contains ~155 chlorophyll *a* and 19 chlorophyll *b*. A decrease from the corresponding ratio of 8.17 to 4.91 needs the addition of 0.98 ± 0.10 LHCII trimers (42 chlorophylls per trimer, for which we measured in *Arabidopsis* an average chlorophyll *a*/*b* ratio of ~1.36), indicating that the

PSI-LHCII preparation was essentially free of other pigment binding complexes. A small contamination due to comigrating ATPase was present, but since this complex does not bind pigments, it did not interfere with any biochemical and spectroscopic measurements performed in this work.

Pigment analyses showed that the PSI preparation had a chlorophyll/carotenoid ratio of 5.17 ± 0.03 (corresponding to 33/34 carotenoids per PSI complex; note that carotenoid molecules were not resolved in the crystal structure of the PSI from pea) and demonstrated the absence of neoxanthin, a carotenoid specifically bound to the PSII antennae. The PSI-LHCII preparation showed a lower ratio (4.84 ± 0.10) due the high carotenoid content of LHCII (12 carotenoids per trimer) and the presence of three neoxanthin molecules per complex when the pigments were normalized to the total chlorophyll content of a PSI-LHCII complex (~215 chlorophylls).

On the basis of the respective chlorophyll contents, it was calculated that the peaks in the Q_y absorption band of PSI-LHCII and PSI preparations should have a ratio of ~1.15 at the same molar concentration. By normalizing the absorptions of the two native preparations using this ratio, we indeed found that the difference between the spectra was almost identical to that of a trimeric LHCII (Figure 2). Note that this result is possible if and only if the preparations are pure, thus giving more evidence of the quality of the purification. Using the spectra normalized to the same molar concentration, it was calculated that the PSI-LHCII absorption cross section in the visible region (350 to 750 nm) was increased by 21% compared with PSI.

Steady State Fluorescence Analysis

PSI and PSI-LHCII were analyzed by steady state fluorescence spectroscopy at 77K. The PSI emission spectrum (Figure 3A) was characterized by the classical far-red fluorescence peak (731 nm). PSI-LHCII complexes showed a very similar emission spectrum, with a small peak around 680 nm where LHCII has its emission maximum. After disassembling the supercomplex (see next section), a clear LHCII fluorescence emission peak was observed around 680 nm due to the fact that detached LHCII cannot transfer its excitation energy to PSI (Figure 3A). This indicates that most of the energy absorbed by LHCII is transferred to PSI before it can be emitted as fluorescence. This was confirmed by the fluorescence excitation spectra measured at the maximum of the PSI emission (Figure 3B): The LHCII contribution in the PSI-LHCII complex compared with the PSI complex was evident and followed closely the absorption difference between PSI-LHCII and PSI (Figure 1).

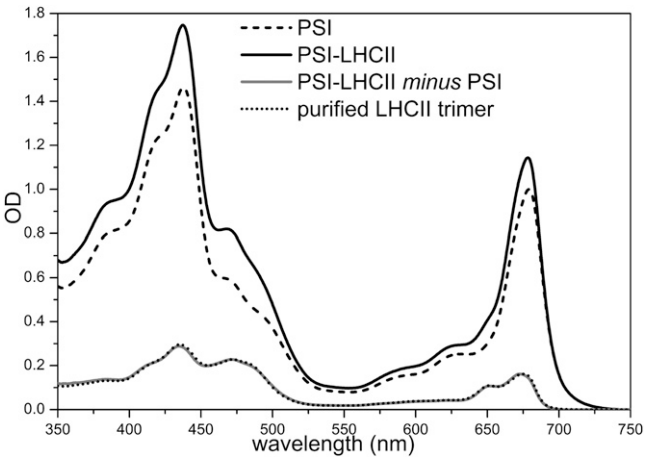

Figure 2. Absorption Spectra of PSI and PSI-LHCII Normalized to the Same Molar Concentration.

The difference spectrum (PSI-LHCII minus PSI) is shown and compared with the spectrum of a purified LHCII trimer. The two spectra are almost identical.

Stability of the PSI-LHCII Supercomplex

The stability of the PSI-LHCII complex was studied by fluorescence kinetics analysis at room temperature during different treatments. At room temperature, PSI and PSI-LHCII fluorescence emission spectra are rather similar (see Supplemental Figure 2 online), and it is not possible to clearly distinguish between PSI and LHCII emission because LHCII bound to PSI is strongly quenched due to effective energy transfer to PSI, which has a very short excited state lifetime (Turconi et al., 1996; Croce et al., 2000; van Oort et al., 2008; and below). However, after its detachment from PSI, the LHCII fluorescence quantum yield increases significantly, as the average excited-state lifetime of free LHCII in solution is ~3 to 4 ns (Moya et al., 2001). Therefore, monitoring the fluorescence increase at 680 nm provides a direct measurement of LHCII detachment from PSI. We tested the PSI-LHCII stability in the presence of detergents and salt and at different temperatures. As shown in Supplemental Figure 3 online, the PSI-LHCII complex showed a strong stability at high salt (0.5 M NaCl) and increased temperature (30°C), a reasonable stability in the presence of a high concentration of digitonin, but instability at a low concentration of α-DM (0.02%) which leads to the rapid detachment of LHCII from PSI. The PSI-LHCII complex was also found to resist freezing and thawing.

Electrophoresis Analyses on S, M, and Mobile LHCII Trimers

To unveil which LHCII complex can be transferred to PSI under State II conditions, the Lhcb isoforms of PSI-LHCII were compared with those of trimers S and M. The Lhcb3 protein is easily detectable on a SDS-PAGE because it migrates in a distinct and lower band well separated from Lhcb1-2. On the contrary, Lhcb1-2 isoforms from *Arabidopsis* (and many other species) migrate in one single band in a gel (Figure 1). For this reason, we also used in this experiment a PSI-LHCII preparation obtained from maize (*Zea mays*): This preparation has the same properties as the one from *Arabidopsis*, but it has the advantage of allowing the separation of the Lhcb1-2 isoforms in few distinct SDS-PAGE bands (De Luca et al., 1999), allowing the determination of a fingerprint of the different kinds of trimers (S, M, and mobile trimers). Analyses of gels with maize samples (Figure 4A) stained with Sypro Ruby and immunoblots from both species (Figures 4B and 4C) showed that the Lhcb3 isoform, which is thought to be exclusively present in trimer M (Hankamer et al., 1997; Boekema et al., 1999b), was barely detectable in

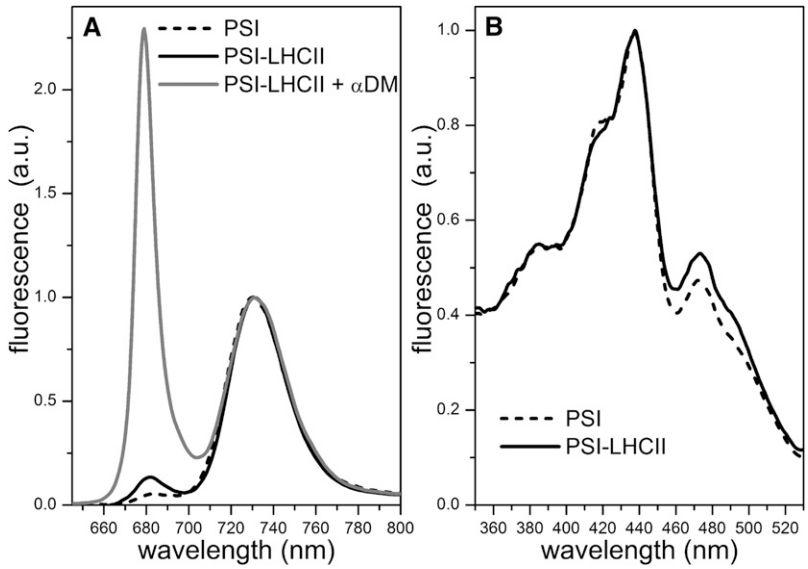

Figure 3. 77K Fluorescence Spectra of PSI and PSI-LHCII Fractions.

(A) Emission spectra of PSI and PSI-LHCII excited at 440 nm and of PSI-LHCII treated with α-DM, which destroys the binding between LHCII and PSI. Spectra were normalized at maximum PSI emission.

(B) Excitation spectra measured at the PSI maximum emission and normalized to the maximum in the Soret region.

a.u., arbitrary units.

the PSI-LHCII supercomplex. Moreover, the relative accumulation of the Lhcb1-2 isoforms of trimer M was different from that of the Lhcb isoforms in PSI-LHCII, thus indicating that trimer M does not, or nearly not, participate in state transitions. The relative accumulation of the Lhcb1-2 isoforms in PSI-LHCII was also different from that of trimer S (Figure 4A), also showing that this trimer is not substantially involved in state transitions.

Note that trimer L, different from trimers S and M, cannot be purified; thus, direct analysis of the LHCII content of this trimer is not possible. However, because trimers S and M are (almost) not involved in state transitions, it is concluded that L trimers loosely associated with PSII (in State I) are the mobile LHCIIs mainly bound to PSI in State II.

Furthermore, the gel with the maize PSI-LHCII complex from maize (Figure 4A) showed an intense band of isoforms migrating in the lower part of the Lhcb1-2 region, indicating that a specific set of Lhcb1-2 isoforms belongs to the mobile LHCII pool. Immunoblot analysis showed that both Lhcb1 and Lhcb2 proteins are involved in state transitions (Figures 4B and 4C).

Mass Spectrometry Analysis of S, M, and Mobile LHCII Trimers

To confirm previous results from SDS-PAGE/immunoblots and to improve the analysis of the isoforms involved in state transition, we performed a direct investigation of the Lhcb1-3 content by mass spectrometry (MS) on the S, M, and mobile trimers from *Arabidopsis*.

A region containing all Lhcb1-3 isoforms was cut from a SDS-PAGE gel loaded with preparations of trimers as in Figure 4C and analyzed by quantitative MS (Szopinska et al., 2011). Different peptides specific for Lhcb1-2-3 isoforms were identified (see Supplemental Figure 4 online) and used for their relative quantification in S, M, and mobile trimers.

Note that in *Arabidopsis*, Lhcb1 proteins are encoded by five genes (*lhcb1.1-5*), Lhcb2 isoforms by four genes (*lhcb2.1-4*), and Lhcb3 by one (Jansson, 1999). Mature Lhcb1.1, 1.2, and 1.3 proteins are identical; Lhcb1.4 and 1.5 have six and three substitutions compared with Lhcb1.1-3, respectively (and 1.4 and 1.5 are different for just three amino acids). Similarly, the four *lhcb2* genes encode for three identical mature proteins (Lhcb2.1-3) and a fourth Lhcb2 that has just three amino acid substitutions (Lhcb2.4) (see Supplemental Figure 4 online). Despite the extreme similarities, MS analyses were able to identify specific peptides for Lhcb1.4 and peptides shared by Lhcb1.4 and Lhcb1-5, while no peptide for a specific Lhcb2.1-4 protein was identified.

Comparison of the relative content of Lhcb1, 2, and 3 isoforms in the S, M, and mobile trimers revealed a significant difference in trimer composition (Figure 5). In particular, LHCII-M was strongly enriched in Lhcb3, in accordance with previous analyses showing approximately one Lhcb3 protein per trimer (Caffarri et al., 2004). LHCII-M was also enriched in Lhcb1 isoforms, while Lhcb2 was almost absent in this trimer compared with mobile and S trimers. Mobile trimer had a similar amount of Lhcb1 isoform as S trimers and a small reduction of Lhcb2 proteins, partially compensated for by a small increase in Lhcb3. Looking at specific Lhcb1 isoforms, it was evident that trimer M had the highest content of the Lhcb1.4 isoform, trimer S the lowest, and the mobile trimer an intermediate level (Figure 5B).

When peptides specific for both Lhcb1.4 and 1.5 were analyzed (Figure 5C), their total relative content in M trimers was

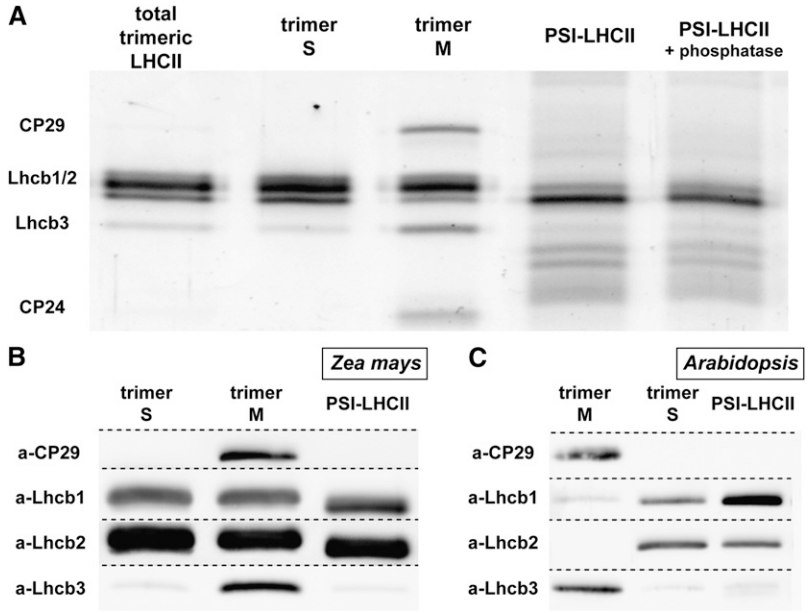

Figure 4. Analysis of Lhcb1-3 Isoforms Involved in State Transitions.

(A) Sypro-stained SDS-PAGE gel of different kinds of LHCII trimers prepared from maize thylakoids. The "total trimeric LHCII" lane is a preparation representative of most of the LHCII present in membranes obtained as band 3 (trimeric LHCII) of a Suc gradient of thylakoids solubilized with 0.6% α-DM; the "trimer S" lane is a preparation enriched in LHCII trimers strongly bound to PSII (S) and was obtained by disrupting a preparation of the CS complex, which is composed of monomeric PSII core/CP26/trimer S (Caffarri et al., 2009), and recovering the trimeric LHCII on a subsequent Suc gradient; the "trimer M" lane is a preparation of LHCII moderately bound to PSII (M), which contains one Lhcb3 per trimer, and was obtained as a supercomplex with CP29 and CP24 (Caffarri et al., 2004); PSI-LHCII was prepared as described in the text; "PSI-LHCII + phosphatase" is the same preparation treated for 2 h with the CIP phosphatase, effective in dephosphorylating LHCII (see Supplemental Figure 8 online), showing that phosphorylation of LHCII does not change its mobility.
(B) Immunoblot analysis of the maize preparations of trimers S, M, and PSI-LHCII shown in **(A)** probed with the anti-Lhcb1, 2, and 3 and CP29 antibodies. The analysis confirms the presence of a very low amount of Lhcb3 bound to PSI. LHCII isoforms reactive to Lhcb1 and 2 antibodies are present in the PSI-LHCII complex. Absence of CP29 in the PSI-LHCII lane indicates that this fraction has no contamination from PSII supercomplexes.
(C) Immunoblot analysis of preparation of trimers M, S, and PSI-LHCII from *Arabidopsis* shows similar results for Lhcb3 and CP29 distribution. In the case of Lhcb1, a low signal is detected in trimer M, which could be due to the low reactivity of the a-Lhcb1 antibody against the isoforms present in this trimer (see Figure 5). In the case of Lhcb2, no signal is detected in trimer M, suggesting the absence or low content of Lhcb2 in LHCII-M of *Arabidopsis*. Both Lhcb1 and 2 are detected in the *Arabidopsis* PSI-LHCII complex.

found to be strongly reduced compared with mobile and S trimers, suggesting that the Lhcb1.5 isoform is a minor component of LHCII-M (Figure 5B). Even if absolute content of Lhcb1.4 isoform was not known, the relative content of Lhcb1.5 between trimers could be easily calculated using a set of fixed values for Lhcb1.4 amount: The results indicate that, independently from the precise Lhcb1.4 content, mobile trimer had the highest content of Lhcb1.5, trimer M the lowest. and trimer S an intermediate level.

Both Lhcb1.4 and Lhcb1.5 were enriched in mobile trimers compared with S trimers, implying that LHCII-S is enriched in Lhcb1.1-3 isoforms compared with mobile trimers.

In conclusion, MS analyses confirm results from SDS-PAGE/immunoblots about the identity of the trimer involved in state transition and add new information about the isoform content of different trimers. Since trimers associated with PSI in State II had a different composition compared with trimers S and M, it can be concluded that mobile LHCII is mainly composed of L trimers loosely associated with PSII in State I.

Fluorescence Decay Kinetics

The measurements of steady state fluorescence emission at 77K indicated that energy transfer from LHCII to PSI is very efficient (Figure 3). However, this analysis did not provide detailed information relative to the kinetics of energy transfer, which determine the yield of photochemical conversion. To investigate this point in further detail, the fluorescence decay kinetics were measured by time-correlated single-photon counting at 10°C, a temperature close to the relevant physiological conditions. The time resolved data were fitted globally, and the decay-associated spectra (DAS) for PSI from plants in State I and for PSI-LHCII from plants in State II are presented (Figures 6A and 6B, respectively). In both preparations, the best fit was obtained by a sum of five exponential components. Two of these lifetimes fell in the interval of 600 to 800 ps and 3.2 to 3.6 ns and, based both on the lifetime and the respective DAS band shape, could be assigned to a very small fraction (1 to 1.5% of the integrated area under the DAS) of uncoupled or

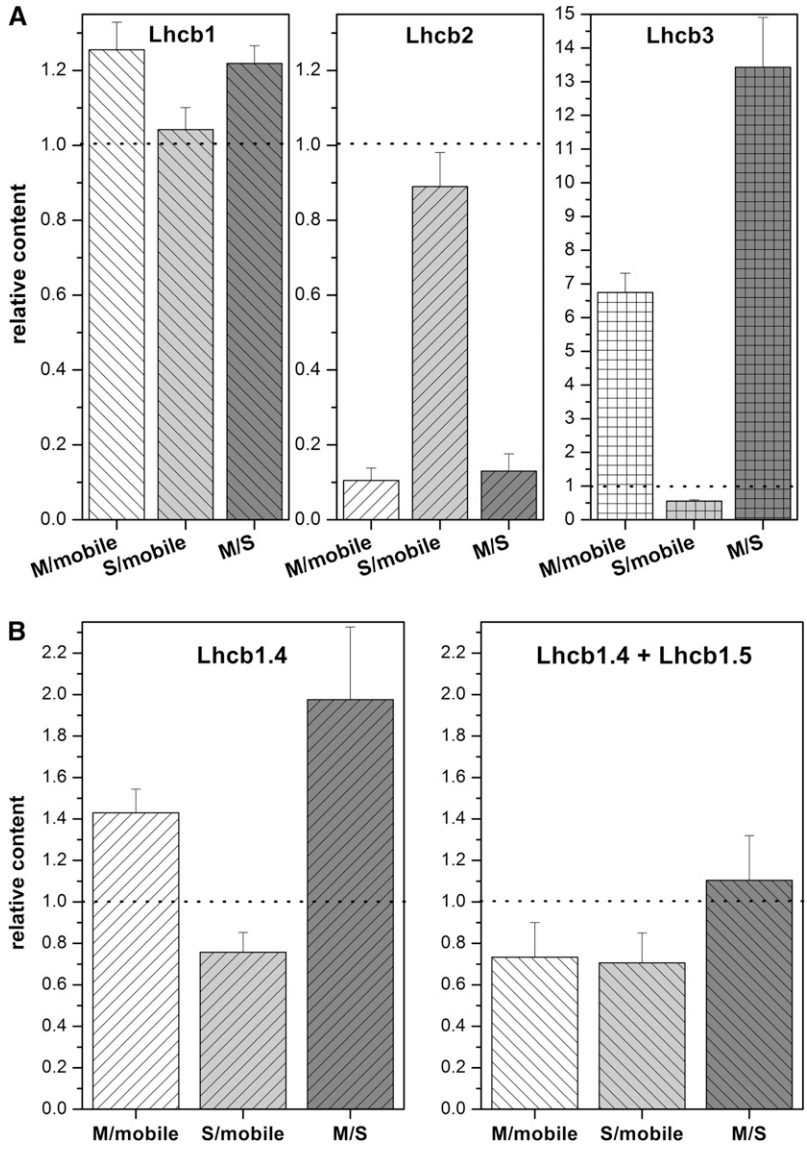

Figure 5. Analysis of Lhcb1-3 Isoforms in M, S, and Trimers Bound to PSI (Mobile) by MS.

Samples are prepared as in Figure 4.

(A) Relative content of total Lhcb1, total Lhcb2, and Lhcb3 as ratio between amounts of each isoform in the three kinds of trimers. M trimer is strongly enriched in Lhcb3, enriched in Lhcb1, and strongly reduced in Lhcb2 compared with mobile and S trimers, implying that LHCII-M is little involved in state transitions.

(B) Relative content of Lhcb1.4 and total Lhcb1.4+1.5 isoforms in M, S, and mobile trimers. Relative content of Lhcb1.4 follows this order: M>mobile trimer>S. Lhcb1.5 relative content in each trimer can be calculated (see text) and follows this order: mobile trimer>S>M. Standard errors are indicated.

weakly coupled chlorophyll-protein complexes. The small amplitudes of these long-lifetime components, which will not be further considered, indicate that practically all complexes in solution can be considered intact. The remaining lifetimes, yielding the description of the energy transfer and trapping in PSI and PSI-LHCII, fell in the 10 to 25 ps, 30 to 50 ps, and ~90 to 110 ps ranges. We note that these descriptions, both in terms of the lifetimes and the DAS band shapes, are rather similar to those obtained previously for different PSI preparations (Croce et al., 2000; Ihalainen et al., 2005; Engelmann et al., 2006). The most straightforward interpretation of the DAS is the following: (1) The 13 to 17 ps decay is dominated by an energy transfer component from the bulk antenna to the long wavelength chlorophyll forms present in LHCI; (2) ~40 and ~100 ps represent decays from the terminal emitter of PSI. Each of these DAS contains different contributions from distinct red forms having emission maxima at ~715 and ~735 nm. Moreover, even though both long-lived lifetimes involve contributions from the 735-nm form, the different lifetimes (~40 and ~100 ps) and DAS band shapes can be explained by two separate and kinetically

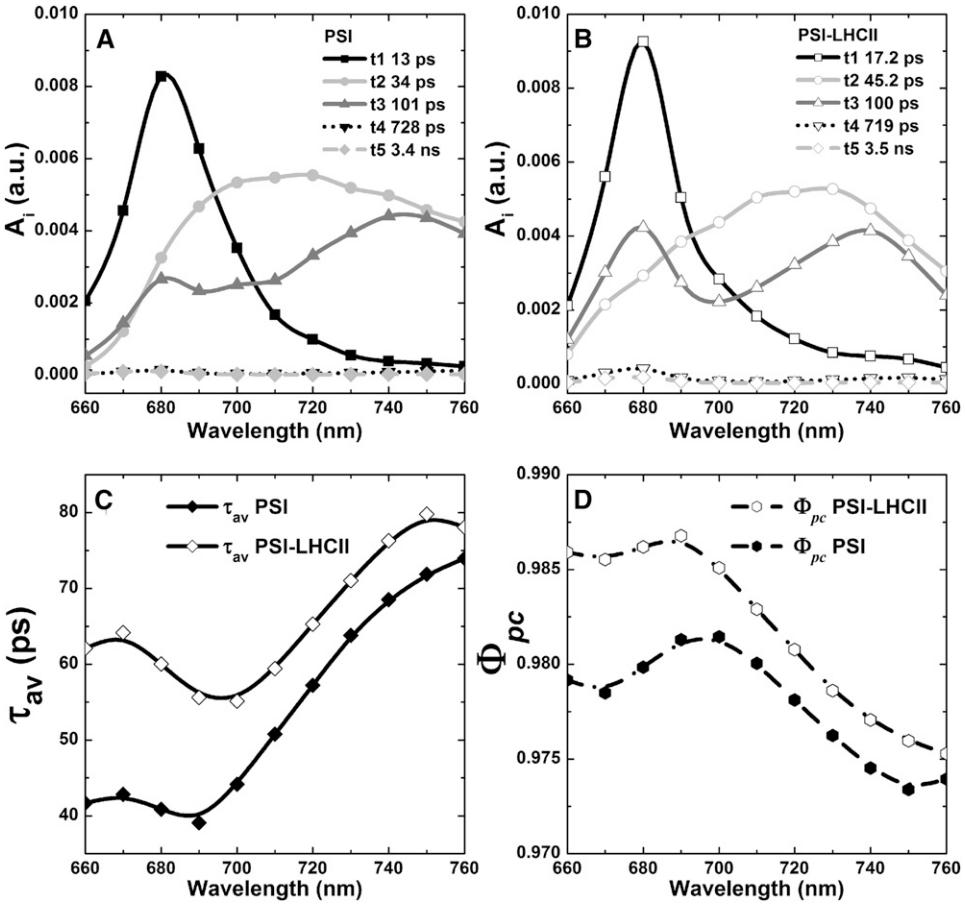

Figure 6. Time-Resolved Fluorescence Analysis of PSI-LHCII and PSI.

(A) and **(B)** Analysis of fluorescence lifetimes in terms of DAS in PSI **(A)** and PSI-LHCII **(B)** supercomplexes. In **(A)**: squares, 13 ± 6 ps; circles, 35 ± 8 ps; up triangles, 101 ± 12 ps; down triangles, 728 ± 145 ps; diamonds, 3.4 ± 0.3 ns. In **(B)**: squares, 17 ± 8 ps; circles, 43 ± 10; up triangles, 100 ± 15 ps; down triangles, 719 ± 180 ps; diamonds, 3.5 ± 0.4 ns. Spectra were normalized to the total area of the three fastest components. The errors are the SD calculated from a minimum of five independent measurements per preparation. a.u., arbitrary units.

(C) Dependence of average lifetimes (τ_{av}) on the emission wavelength. Closed diamonds, PSI; open diamonds, PSI-LHCII.

(D) Dependence of the maximal photochemical quantum efficiency (Φ_{pc}) on the emission wavelength. Closed circles, PSI; open circles, PSI-LHCII.

distinct 735-nm populations (Engelmann et al., 2006). It is possible that this kinetic heterogeneity is associated with the presence of a long-wavelength chlorophyll form in each of the two LHCI dimers (Lhca1-4 and Lhca2-3), as has been recently reported by Wientjes and Croce (2011). It is evident that the lifetimes do not vary significantly in the PSI-LHCII supercomplex compared with PSI, especially when the uncertainties associated with the fit parameters, and intersample variability, are taken into account. For instance, the 13 ± 6 ps and 35 ± 8 ps lifetimes in PSI varied only slightly in PSI-LHCII, where they became 17 ± 8 ps and 43 ± 10 ps, whereas the longer lived components had the values of 100 ± 15 ps in both preparations. The overall shapes of the DAS were substantially maintained in both complexes, but for the PSI-LHCII complex, it is interesting to note an increase in the relative amplitude of the ~40 and ~100 ps components with respect to the ~10 ps one in the 670- to 690-nm interval, where the LHCII decay occurs (this point will be taken up below). Thus, from inspection of the fit results it emerges that energy transfer between LHCII and PSI in the supercomplex is fast. This is also demonstrated by the fact that in the case of weak or moderate coupling of the LHCII moieties to PSI, one would expect to observe an additional decay component associated with this energy transfer process, which is not present in the experimental results.

As mentioned above, moderate increases in the ~40- and ~100-ps components in the 670- to 690-nm interval for the PSI-LHCII complex were observed. To analyze this aspect further, we determined the value of the average lifetime ($\tau_{av} = \sum A_i\tau_i / \sum A_i$), a parameter that allows calculation of the effective trapping time ($\tau_{av} \approx K_{pc}^{-1}$) across the emission band for both PSI and PSI-LHCII. The results are shown in Figure 6C in terms of the τ_{av} parameter. As observed in previous investigations on isolated PSI, there was a marked variation of the value of τ_{av} across the emission band, with highest values being detected in the emission tail, which is dominated by the long wavelength chlorophyll forms (Croce et al., 2000; Jennings et al., 2003;

Engelmann et al., 2006). This finding, which was also apparent in the PSI-LHCII supercomplex, was interpreted in terms of a partial diffusion limitation to trapping imposed by uphill energy transfer from the red forms to the photochemical trap (Jennings et al., 2003). Interestingly, whereas in the tail of the spectrum ($\lambda > 710$ nm), the values of τ_{av} in PSI and PSI-LHCII supercomplexes were substantially the same, within the measurement errors, significant differences were observed in the 670- to 690-nm interval, where the LHCII contribution is most pronounced. In this interval, τ_{av} increased from 42 ps in PSI to 60 ps in PSI-LHCII.

To understand the impact of these variations in the trapping kinetics in PSI-LHCII compared with PSI, we estimated the yield of photochemical trapping (Φ_{pc}) across the emission band (see Methods). To determine Φ_{pc} it was also necessary to have an estimate of the constants associated with the so-called trivial deexcitation processes of the singlet excited state ($\tau_d^{-1} = \sum k_j$, where j represents fluorescence, internal conversion,^{j} intersystem crossing, etc.). As the fluorescence decay in PSI is almost independent of the redox state of electron donor (Byrdin et al., 2000), information concerning these processes, which could be determined under conditions of so-called "closed" reaction centers (as for PSII), is not readily available. We therefore used the values obtained for the isolated LHCI (τ_{LHCI}), the external antenna complexes of PSI, as an approximation for the excited state decay in the absence of photochemical quenching (i.e., $\tau_d \approx \tau_{LHCI}$). As the value of τ_{LHCI} measured in the isolated LHCI antenna varies in the literature from 2.5 to 3.8 ns (Gobets et al., 2001; Engelmann et al., 2006; Wientjes et al., 2011), we used these figures to estimate the lower and higher limits of Φ_{pc}, both for PSI and PSI-LHCII, and the mean values are shown as a function of wavelength in Figure 6D. It should be pointed out that an error as large as 1 to 2 ns in τ_d would have only a minor effect on the efficiency determined and in no way modify any of our conclusions.

The quantum efficiency of PSI determined in this fashion was amazingly high, with a maximal value of 0.986 $\pm$ 0.05 at shorter wavelengths and of 0.975 ($\pm$ 0.05) in the red tail of the emission for the case of PSI. Previous data using the same instrumentation and another PSI preparation yielded efficiency values closer to 0.95 (Jennings et al., 2003). The presence of LHCII in the supercomplex brought about only a slight reduction of the maximal quantum efficiency Φ_{pc} (0.980 $\pm$ 0.05) in the blue wing of the spectrum in the PSI-LHCII supercomplex, which is where LHCII contributes significantly, whereas very similar yields were determined for these preparations at long emission wavelengths (Figure 6D). Thus, the attachment of an additional LHCII trimer to PSI reduces the photochemical efficiency by <1%.

PSI and LHCII Interaction Analyzed by Circular Dichroism Spectroscopy

The fact that besides ultrafast EET within the individual pigment-protein complexes, ultrafast transfer also occurs between LHCII and PSI suggests that excitonic interactions might occur also between pigments in different complexes, as occurs between pigments within individual complexes. Circular dichroism (CD) can be a useful technique to detect such interactions (Georgakopoulou et al., 2007; Garab and van Amerongen, 2009). Therefore, CD spectra of PSI-LHCII complexes were compared with the sum of the spectra of the isolated complexes. In addition, the PSI-LHCII complexes were measured before and after disrupting their mutual interaction with a low amount of α-DM (see stability section). In both cases, a clear and similar CD difference spectrum with a negative peak in the chlorophyll *a* region (674/676 nm) was observed (Figure 7; see Supplemental Figure 5 online), suggesting the presence of excitonic interaction between chlorophyll *a* in PSI and LHCII.

EM

EM analysis was performed not only to try to improve previously proposed structural models of PSI-LHCII (Kouril et al., 2005; Amunts et al., 2007), but also to search for the possible existence of other PSI-LHCII particles, since previous analyses were performed on a heterogeneous preparation of solubilized thylakoids, and less abundant PSI-LHCII complexes with a different structural organization were possibly not noticed (Kouril et al., 2005).

EM analysis of the PSI-LHCII fraction shows the presence of only one kind of particle (Figure 8; see Supplemental Figure 6 online), and, given the stoichiometry of 1:1 between PSI and LHCII, this suggests that trimeric LHCII is always bound to PSI at one specific position. On the basis of the obtained EM density map, the LHCII crystal structure (Liu et al., 2004), and the recently updated PSI structure (Amunts et al., 2010), a structural model of the PSI-LHCII supercomplex was constructed (Figure 8). The fitting of the EM map with the x-ray structure of PSI was based on the white spots on the center-left part and the dark densities in the center-lower part of the complex that are unequivocally associated with protruding mass (part of PsaD, C, and E from up to low) and cavities (gap between Lhca and core), respectively, identifiable in the crystal structure. For an optimal fit, a small rotation of PSI was needed (right side up).

For LHCII, density spots could not be easily associated with specific features, and they were also different from the ones previously identified for PSII-LHCII supercomplexes (Caffarri et al., 2009), since PSI and PSII were viewed from different sides (stromal and luminal sides, respectively). However, LHCII could be positioned based on its triangular shape when projected over the membrane plane, which could be superimposed on the same shape present in the PSII supercomplex (Caffarri et al., 2009). Moreover, the presence of additional chlorophylls in the new PSI structure (Amunts et al., 2010) required a small displacement of LHCII with respect to PSI as compared with previous models (Kouril et al., 2005; Amunts et al., 2007). In conclusion, the orientation and position of LHCII in our updated structural model of the PSI-LHCII supercomplex are slightly different from what was previously suggested, and we propose that LHCII transfers its excitation energy from chlorophylls 611 to 612 (the lowest energy chlorophylls in LHCII; Remelli et al., 1999) toward chlorophyll 11145 on PSI, a chlorophyll recently identified in the crystal structure.

DISCUSSION

Energy partitioning between PSII and PSI has been a subject of investigations for many years (Bennett et al., 1980; Allen et al.,

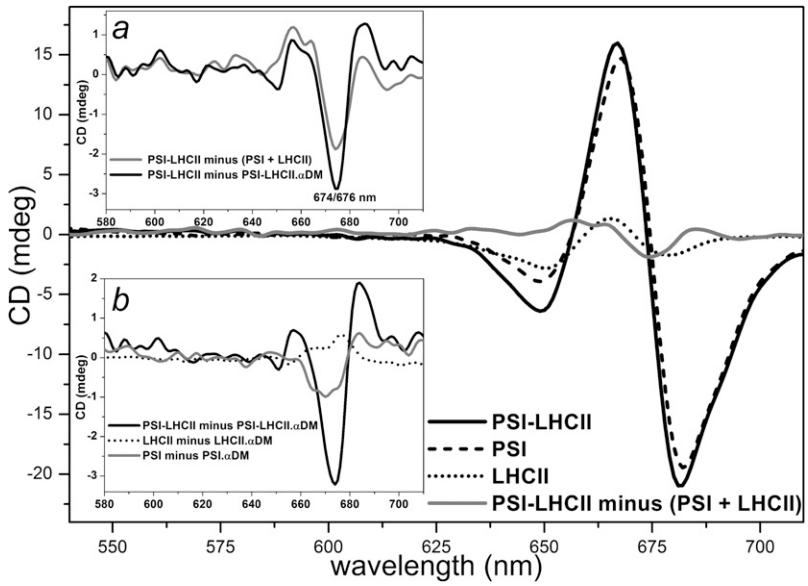

Figure 7. CD Spectra of PSI, PSI-LHCII, and LHCII from Maize Prepared in Digitonin.

The spectra were normalized to the same molar concentration (main graph). A specific CD signal due to the interaction between PSI and LHCII was identified by (1) comparison of isolated PSI, LHCII, and PSI-LHCII complexes; and (2) comparison of intact and dissociated PSI-LHCII complexes. The difference spectrum "PSI-LHCII" minus ("PSI" + "LHCII") is shown in the main graph and also in inset a; the difference spectrum of PSI-LHCII before (intact complex) and after treatment with 0.02% α-DM (to disrupt LHCII to PSI binding) is shown in inset a. The same detergent treatment on purified PSI and LHCII (shown in inset b, together with the difference spectrum "PSI-LHCII" minus "PSI-LHCII after α-DM treatment") had a very small effect on single PSI and LHCII complexes. The two approaches on maize preparations (here) and *Arabidopsis* (see Supplemental Figure 5 online) gave very similar negative CD signals (peaks at 674/676 nm, respectively) originating in the interaction between PSI and LHCII.

1981). Moreover, genetic approaches have recently allowed the identification of key proteins involved in state transitions, such as the kinases and phosphatases regulating the phosphorylation state of LHCII and its relocation between PSII and PSI (Bellafiore et al., 2005; Pribil et al., 2010; Shapiguzov et al., 2010). Recent biochemical and physiological studies have given information on the mechanism and importance of state transitions in plants (Tikkanen et al., 2006; Tikkanen et al., 2010). Studies on the green alga *C. reinhardtii* have indicated important differences in algae with respect to plants, such as the participation of the monomeric antennae CP26 and CP29 in state transitions in this green alga (Takahashi et al., 2006; Iwai et al., 2008). However, so far very little is known about the properties of the plant PSI-LHCII complex formed during State II conditions.

The main issue that has hampered the study of PSI-LHCII was the purification of this supercomplex, which was considered to be quite unstable after the detergent treatment necessary for thylakoid solubilization and protein extraction (Zhang and Scheller, 2004; Kouril et al., 2005). Recently, purifications of PSI-LHCII complexes from *C. reinhardtii* and spinach were reported (Takahashi et al., 2006; Qin et al., 2011), but in both cases very little biochemical and spectroscopic characterization was performed. The complexes were purified with β-DM and α-DM as detergents, conditions in which the *Arabidopsis* and maize PSI-LHCII complexes are not stable. By making use of the large and bulky detergent digitonin, we now managed to obtain a pure PSI-LHCII preparation in solution that was stable under many conditions. However, when we added α-DM, which is a mild detergent as well but smaller and with a long aliphatic chain, the intercomplex interactions between LHCII and PSI were disrupted. This property enabled us to investigate the interaction between LHCII and PSI (Figures 3A and 7; see Supplemental Figure 3 online).

Energy Transfer from LHCII

By performing steady state and time-resolved fluorescence spectroscopy, it was possible to study EET from LHCII to PSI. LHCII bound to PSI increases the absorption cross section in the visible region by 21%, and, as shown by steady state fluorescence measurements at 77K, the energy absorbed by LHCII is efficiently transferred to PSI. Time-resolved fluorescence measurements at 10°C and DAS analyses showed that excited state transfer from LHCII to PSI core occurs on a tens of picoseconds timescale, indicating that energy transfer to PSI is also fast.

Excitonic interactions between chlorophyll *a* of LHCII and PSI are also suggested by the appearance of a CD signal at 674/676 nm after the formation of the PSI-LHCII complex. Moreover, time-resolved measurements also allowed the computation of the trapping efficiency of the PSI-LHCII complex compared with that of PSI at physiological temperatures. The calculation indicated that the attachment of an additional LHCII trimer to PSI reduces the photochemical efficiency by <1%. Hence, from a biological point of view, under State II conditions, the quantum efficiency of PSI is virtually unaltered compared with State I, and

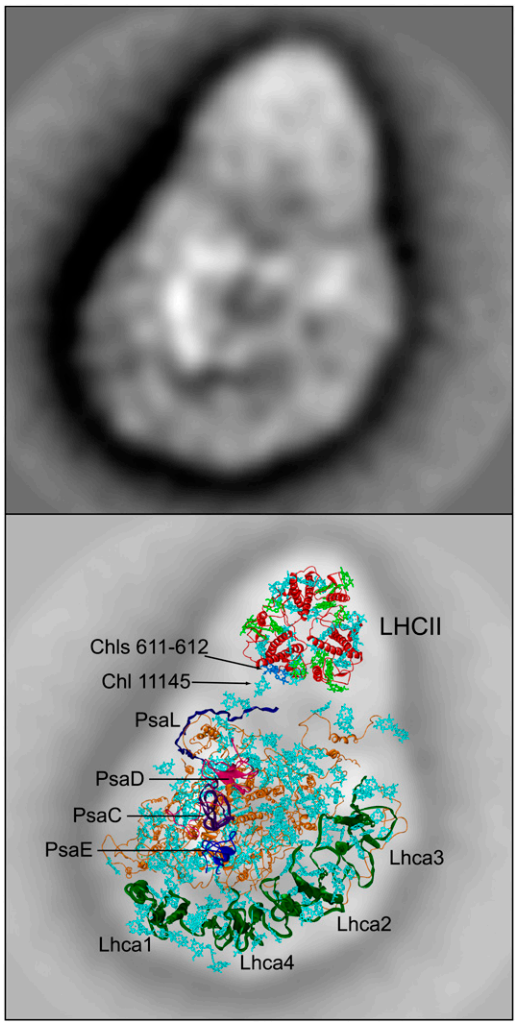

Figure 8. EM Map and Structural Model of the PSI-LHCII Supercomplex.

Lhca complexes are indicated in dark green and are located on the opposite site of LHCII. In PSI, chlorophylls *a* and *b* are indicated in cyan. In LHCII, chlorophylls *a* are indicated in cyan and chlorophylls *b* in green. The stromal protruding proteins PsaD, C, and E and the PsaL subunit (important for the LHCII docking site) are also shown. Note that the docking site for LHCII is not well resolved in the crystal structure; therefore, PSI polypeptides lacking in the crystal structure (in particular the PsaO and PsaP subunits) would probably fill part of the space between LHCII and PSI.

this small negligible decrease is largely compensated for by the increased probability of photon absorption due to the larger cross section of the photosystem.

This finding serves as strong support for the role of the mobile LHCII as a PSI antenna under State II conditions.

PSI-LHCII Structural Model

The two-dimensional projection hybrid map of the PSI-LHCII structure that is presented here, based on the EM density map (Figure 8) and the crystal structures of PSI (Amunts et al., 2010) and LHCII (Liu et al., 2004), strongly suggests that chlorophylls 611 and 612 in LHCII transfer energy to the recently identified chlorophyll 11145 in PSI. It is worth noting that chlorophylls 611 and 612 represent the lowest-energy state in LHCII (Remelli et al., 1999). The same chlorophylls are involved in intercomplex energy transfer within the PSII supercomplex (Caffarri et al., 2009). The energy transfer from LHCII to PSI on the right side of the LHCII complex (Figure 8) is likely to be less important, since in this case the contact would involve high-energy chlorophylls *b* that have a lower excited state population probability at equilibrium.

The chlorophyll 11145 appears to be floating in the PSI structure since the low resolution of this crystal domain has not allowed resolving the amino acid chains; therefore, its existence was questioned (Amunts et al., 2010). However, its position makes it ideal for energy transfer from LHCII to PSI. It cannot be excluded that also other chlorophylls not resolved in the structure are present in this region of PSI, which would further facilitate fast energy transfer.

Trimers Involved in State Transition

The identity of the mobile LHCII trimers involved in state transitions was so far a debated and open question (Bassi et al., 1988; Kouril et al., 2005; Damkjaer et al., 2009). Moreover, recently a new mechanism for state transitions has been proposed (Tikkanen et al., 2008; Järvi et al., 2011): Instead of LHCII being transferred to the stroma lamellae, PSI would approach the grana margins where, after some reorganization of this thylakoid region, it would associate with PSII supercomplexes such that the energy absorbed by PSII could flow to the faster-working PSI complex (spillover).

In our work, we did not find evidence for the occurrence of PSI-LHCII-PSII megacomplexes under State II conditions (Figure 1; see Supplemental Figure 1 online). In the recent report on the identification of this megacomplex (Järvi et al., 2011), the absence of thylakoids in State I as a control (to exclude unspecific aggregation) does not allow an unequivocal conclusion. Note that the purification of such a complex would be possible only if the LHCII involved in PSI binding would also be stably bound to PSII, such as trimer S or M (both trimers show binding that is at least as strong as the one between LHCII and PSI, since they resist α-DM solubilization; Caffarri et al., 2009). The absence of these megacomplexes in our work (see Supplemental Figure 1 online) are in agreement with our analyses on LHCII isoforms bound to PSI, which strongly indicate that trimers participating in state transitions are principally the ones loosely and peripherally bound to PSII, whereas trimers S and M are not significantly involved (Figures 4 and 5).

A small amount of Lhcb3, considered to be exclusively present in trimer M (Hankamer et al., 1997; Boekema et al., 1999b), was detected in PSI-LHCII. This can be explained by the participation of a few M trimers in state transitions as was proposed before (Kouril et al., 2005), although the presence of some Lhcb3 in other trimers also cannot be completely ruled out. Interestingly, it was recently found that replacement of Lhcb3 by Lhcb1-2 in *lhcb3* knockout plants weakens the connection of trimer M (Caffarri et al., 2009; Damkjaer et al., 2009)

and accelerates the rate of state transitions (Damkjaer et al., 2009). Damkjaer et al. suggested that M trimers participate more in state transitions in the mutant compared with wild-type plants, thus suggesting that Lhcb3 has a function in locking this trimer to PSII. The low amount of Lhcb3 bound to PSI found in this work supports the proposition.

Interestingly, two other mutants, one lacking PsbW (García-Cerdán et al., 2011), the other lacking Psb27 (Dietzel et al., 2011), both displaying weakened interactions between S/M trimers and the core of PSII, also show faster kinetics of state transitions. On this basis, it has been proposed that that the release of the PSII supercomplexes appears to be the rate-limiting step during state transitions (Dietzel et al., 2011). Yet, based on the same experimental evidence, it may also be proposed that, in these mutants, the presence of more loosely bound trimers (since M and S are less stably associated to the core) makes these trimers mobile, thus increasing the pool of LHCII engaged in state transitions, and, as a consequence, making the process faster. Therefore it could be suggested that, in wild-type plants, the S and M trimers play a minor role in state transitions, but could become more significant if their binding to PSII is weakened, as observed in mutant for PsbW, Psb27, and Lhcb3. From a stoichiometry point of view, loosely bound trimers, which compose almost 50% of total trimers in plants grown under nonsaturating light, are indeed largely sufficient for state transitions, since the process mobilizes ~20% of the entire LHCII pool (Allen, 1992).

Moreover, by looking at native gels in Dietzel et al. (2011), the amount of small PSII supercomplexes, which contain S but not M trimers (the first two lower bands [i.e., C_2S and C_2S_2], described as B8 and B9 bands in Caffarri et al. [2009] and visible in Supplemental Figure 1A online) remains significant in State II. Dietzel et al. (2011) clearly demonstrated that PSII supercomplex stability is reduced after core subunit phosphorylation. However, it is possible that the changes in supercomplex relative amount in the gel are the result of an increased sensitivity of the supercomplexes to the solubilization conditions used in the study (1% β-DM), so that the results presented by Dieztel et al. somehow enhance the alterations occurring in vivo caused by the weaker interactions between the core and the Lhcs. At the same time, such weakened interaction would not necessarily lead to an extensive remodeling in vivo comparable to that proposed for *C. reinhardtii* (Iwai et al., 2008), in which up to 80% of the LHCII can be mobilized. In our native gels using a much softer and partial solubilization of thylakoid with digitonin (see Supplemental Figure 1A online), we did not detect a difference in PSII supercomplex distribution between State I and II membranes.

Thus, by considering our results (Figures 4A and 5), the possibility of differently interpreting previous reports (Dietzel et al., 2011; García-Cerdán et al., 2011), the fact that trimer S has a fundamental role in PSII structure (Dekker and Boekema, 2005; Caffarri et al., 2009), and that the minimum PSII antenna size includes S-LHCII (Morosinotto et al., 2006), we consider that S trimer detachment from PSII during state transition is rather unlikely and could have, at best, a limited impact on the whole process under physiological conditions.

Even if we cannot exclude that a functional PSI-LHCII-PSII interaction exists in vivo, from our results, such a megacomplex would be maintained by very weak interactions (those between PSII and L trimers) that do not resist our very mild solubilization (see Supplemental Figure 1A online). Considering that we have no evidence for the existence of PSII-LHCII-PSI megacomplexes and this is also in contrast with old and recent results showing the absence of energy spillover from PSII to PSI (Butler, 1978; Williams and Allen, 1987; Ruban and Johnson, 2009), we propose an updated model for state transitions integrating our results and recent findings about PSI in State II (Tikkanen et al., 2008): PSI would stably bind a specific set of mobile LHCII trimers that, being peripherally and loosely associated with PSII, are relocated in State II near the grana margins where PSI involved in state transitions is found (Tikkanen et al., 2008). This scenario is very different from state transitions in the green alga *C. reinhardtii*, where PSII is largely reorganized under State II conditions allowing the transfer also of the minor antennae CP26 and CP29 to PSI (Iwai et al., 2008).

Our analyses show that mobile LHCII is composed of a specific set of Lhcb1-2 isoforms. In particular, MS analyses show clear differences in the isoform compositions of different trimers, such as an enrichment of Lhcb1.4 in M trimer (as well in Lhcb3, accompanied by a very low content of Lhcb2), an enrichment of Lhcb1.5 in mobile trimers, and of Lhcb1.1-3 in S trimers. These findings indicate a reason for the existence of a large Lhcb1-3 gene family: Whereas the function of light harvesting is similar in different isoforms (Caffarri et al., 2004; Frigerio et al., 2007), the few amino acid substitutions in specific isoforms may allow the building of PSII supercomplexes containing trimers that occupy different positions (and therefore interact with different proteins) and that need different regulations, such as their mobilization under State II conditions.

It is interesting to note that EET from peripheral LHCII trimers to the PSII core under State I conditions is much slower than EET from the same trimer to the PSI core when bound together under State II conditions. Whereas the S and M trimers transfer excitation energy to the PSII core in tens of picoseconds (Broess et al., 2008; Caffarri et al., 2011), the corresponding time for peripheral trimers is on the order of hundreds of picoseconds (van Oort et al., 2010; Caffarri et al., 2011). Indeed, the overall average trapping time of PSII increases from ~150 ps in the absence of peripheral trimers to more than 300 ps in their presence (van Oort et al., 2010; Caffarri et al., 2011), whereas the overall average trapping time of PSI-LHCII is a few picoseconds longer compared with PSI alone.

Therefore, in contrast with the common view, it might be equally or even more appropriate to consider the mobile pool of LHCII as an intimate part of the PSI antenna system that is displaced to PSII under State I conditions. It should be noted that, even if State I to State II transition is usually considered a photosynthetic regulation working at low light intensities (Rintamäki et al., 2000), plants exposed to full sunlight have been found in State II (Mctavish, 1988), as have plants grown in high light growth chamber conditions (Tikkanen et al., 2006). Since the importance of state transition in nature is not fully understood, future investigations based on the biochemical purification of the PSI-LHCII complex as in our work will allow a better elucidation of the thylakoid state in real field conditions.

In summary, purification of a stable PSI-LHCII supercomplex has allowed the investigation of its biochemical composition and

energy transfer properties at low and at physiological temperatures. It was found that S and M trimers are little involved in state transitions, whereas the peripheral trimers loosely bound to PSII are the main components of the mobile pool of LHCII during state transitions. Moreover, we found that each trimer has a peculiar isoform composition. EET from LHCII to PSI in a PSI-LHCII supercomplex is extremely efficient and much faster than EET from the same trimers to PSII cores under State I conditions; the newly proposed structural model of the PSI-LHCII complex suggests that the lowest-energy pigments chlorophylls 611 and 612 in LHCII transfer excitation energy to chlorophyll 11145 on PSI.

METHODS

Thylakoid Membrane and PSI-LHCII Isolation

Stacked thylakoid membranes were prepared from *Arabidopsis thaliana* and maize (*Zea mays*) leaves grown at 100 μmol m^{-2} s^{-1} at 21°C, using a similar procedure as described (Caffarri et al., 2009), but stopping the preparation before the Triton solubilization used for grana membrane preparation. The State II condition was induced on chloroplasts in solution B1 (solution of ground leaves after filtration) in the presence of 30 μM dibromothymoquinone and 10 mM sodium fluoride (phosphatase inhibitor) in moderate light (~100 μmol m^{-2} s^{-1}) and during moderate shaking for 30 min. The 77K fluorescence emission spectra of thylakoid membranes used in this work are shown in Supplemental Figure 7 online.

For solubilization, 150 μg (in chlorophylls) of stacked membranes was solubilized by adding an equal volume of a solution containing 1% digitonin to 0.2% α-DM to have a final chlorophyll concentration of 0.5 mg/mL, vortexing for a few seconds and incubating 20 min on ice. The solubilized samples shown in Figure 1 were fractionated by ultracentrifugation on a Suc gradient containing in a SW41 rotor, for 17 h at 41,000 rpm (208,000 average relative centrifugal force) and 4°C. Gradients were formed directly in the tube by freezing and thawing a 0.75 M Suc solution containing 0.02% digitonin and 10 mM HEPES pH 7.5. Different Suc concentrations (0.6 to 1 M) can be used to change the time and the separation of different complexes.

Fractions containing PSI and PSI-LHCII were concentrated/diluted/concentrated using a solution of 0.02% digitonin and 10 mM HEPES, pH 7.5 (in order to remove excess Suc), and loaded on a second gradient identical to the first one. Harvested complexes were directly used for measurements or rapidly frozen in liquid nitrogen.

Spectroscopy

Absorption spectra were recorded using a Cary300 (Varian). Steady state 77K fluorescence spectra were recorded with a Cary Eclipse fluorimeter (Varian) by placing the sample in a glass Pasteur pipette at an OD of ~0.05 (red peak) in a final solution with 85% (w/v) glycerol, 10 mM HEPES, pH 7.5, and 0.02% digitonin, cooled in liquid nitrogen.

CD spectra were recorded in the same solution as in the gradient on an AVIV 62ADS spectropolarimeter for *Arabidopsis* samples and on a Jasco J-810 spectropolarimeter for maize samples. Results were almost identical, apart from a shift of ~2 nm of the differential band in the red region (Figure 7, inset a) most likely due to differences in the biological sample (e.g., *Arabidopsis* PSI absorption maximum is shifted +1 nm compared with maize PSI).

Pigment Analysis

The pigment complement of the complexes was analyzed by fitting the acetone extract spectrum with the spectra of the individual pigments (Croce et al., 2002) and by HPLC (Campoli et al., 2009).

Gel and Immunoblot Analysis

SDS-PAGE electrophoresis was performed as described (Laemmli, 1970) but using an acrylamide/bis-acrylamide ratio of 75:1 and an acrylamide+bis-acrylamide concentration of 15.5%. Urea (6 M) was also incorporated into the gels. Gels were loaded with 0.1 μg (in chlorophylls) of LHCII and stained with Sypro Ruby. Immunoblots were performed using Agrisera antibodies.

MS Analyses

Arabidopsis Lhcb1-3 proteins of S, M, and mobile trimers were collected from a polyacrylamide Sypro Ruby stained gel as presented in Figure 4. Proteins were digested with trypsin, labeled with isobaric tags, and analyzed by liquid chromatography–tandem MS spectroscopy according to the method described (Szopinska et al., 2011). Quantification of peptides specific for different isoforms was performed with iTRAQ technology (isobaric tags for relative and absolute quantitation).

To identify specific or common peptides for each Lhcb isoform and to evaluate their relative quantity in S, M, and mobile trimers, the data were analyzed the Protein-Pilot software using the National Center for Biotechnology Information protein sequence database. Based on this treatment, only peptides with >96% confidence were chosen for further analysis and calculations of isoform relative amount in S, M, and mobile trimers. Sequence coverage and number of peptides are indicated in Supplemental Figure 4 online.

To eliminate eventual artifacts due to inequality of total Lhcb protein amount in each sample, all data were normalized on a region showing identical sequence in all isoforms (see Supplemental Figure 4 online). Finally, specific peptide tag peak areas were used for relative quantification of each isoform, and data are presented as M/mobile and S/mobile and M/S trimer ratios.

EM and Single-Particle Analysis

PSI-LHCII complexes were repeatedly diluted (with 0.02% digitonin and 10 mM HEPES, pH 7.5) and concentrated to remove the Suc from the gradient solution. The complexes were negatively stained with 2% uranyl acetate on glow discharged carbon-coated copper grids. EM was performed on a Philips CM120 electron microscope equipped with a LaB_6 tip, operated at 120 kV. Images were recorded with a Gatan 4000 SP 4K slow-scan charge-coupled device camera at 80,000× magnification with a pixel size of 0.375 nm at the specimen level after binning the images. GRACE software was used for semiautomated specimen selection and data acquisition. Single particles were selected with an 80 × 80 pixel frame and analyzed with the Groningen Image Processing software package, with multireference procedures and multivariate statistical analysis and classification (Oostergetel et al., 1998).

Fluorescence Decay Measurements

The fluorescence decay was measured using the time-correlated single-photon counting technique using a home-built apparatus, which has been previously described (Engelmann et al., 2005; Tumino et al., 2008) and has a temporal resolution of ~10 ps after deconvolution of the instrumental response function.

The sample cuvette had a 3-mm path length, and the sample concentration was 0.1 OD/cm at 680 nm, in a buffer containing 10 mM HEPES, pH 7.5, and 0.015% digitonin. Ascorbate (500 μM) and 2,6-dichlorophenolindophenol (20 μM) were present to ensure the reaction centers remained in the so-called open state (reduced primary donor) during data acquisition. All measurements were performed at 10°C.

Data Analysis

Fluorescence decay kinetics, acquired between 670 and 760 nm at 10-nm intervals, were fitted using a global routine based on iterative convolution

of the instrument response function and a decay function represented by a sum of exponentials of the form $F(\lambda,t) = \sum A_i(\lambda)\cdot\exp[-\tau_i/t]$. The lifetimes τ_i are global parameters, whereas the amplitudes $A_i(\lambda)$ that describe the DAS are local parameters in the fit. The instrument response function was determined using a reference dye (DCI'; Exciton) with a known lifetime of ~20 ps, as previously described (Zuker et al., 1985; Tumino et al., 2008), that was directly estimated by the fluorescence decay measurements during the fitting process. The advantages of this method were previously discussed (Tumino et al., 2008). The fitting algorithm, which is based on the Minuit library from CERN, distributed with a C-fortran interface as C-minuit, minimizes χ^2 also allows for the error analysis. The data presented are weighted means of five independent measurements, fitted independently.

Determination of the Effective Trapping Constant and Quantum Efficiency

The trapping time is proportional to the inverse value of the average decay time defined as:

$$\tau_{av}(\lambda) = \frac{\sum_i A_i(\lambda)\cdot\tau_i}{\sum_i A_i(\lambda)} \approx {K_{pc}}^{-1}$$

where K_{pc} is the macroscopic (photosystem) photochemical rate constant (not the intrinsic microscopic charge separation rate) from which it is possible to estimate the photochemical quantum efficiency (Φ_{pc}), defined as:

$$\Phi_{pc} = \frac{K_{pc}}{K_{pc} + \sum_i k_i} \approx \frac{\tau_{av}^{-1}}{\tau_{av}^{-1} + \tau_d^{-1}}$$

where $\sum k_i = {\tau_d}^{-1}$ is the sum of the excited state decay process (excluding photochemistry), which is typically determined for PSII at so-called closed reaction center. For PSI, this information is not available because closed reaction centers are strong fluorescence quenchers. Therefore, we used different values derived from the isolated external antenna LHCI ($\tau_d = \tau_{av}[LHCI]$), as a reference. As these values may be approximate, we have taken into account the spread of values in the literature ranging from ~2.5 ns (Gobets et al., 2001; Wientjes et al., 2011) up to 3.5 ns (Engelmann et al., 2006), which result in lower and upper limits for the estimate of photochemical quantum efficiency.

Supplemental Data

The following materials are available in the online version of this article.

Supplemental Figure 1. Analysis of the PSI Oligomeric State by Thylakoid Solubilization and Fractionation on Native PAGE and Suc Gradient.

Supplemental Figure 2. Steady State Fluorescence Emission Spectra at Room Temperature for PSI and PSI-LHCII Preparations.

Supplemental Figure 3. Analysis of the Stability of the PSI-LHCII Complex.

Supplemental Figure 4. Sequence Alignment of Lhcb1.1-5, Lhcb2.1-4, and Lhcb3 Isoforms of *Arabidopsis* and Sequence Coverage by Mass Spectrometry Analysis.

Supplemental Figure 5. Circular Dichroism Spectra of PSI, PSI-LHCII, and LHCII from *Arabidopsis*.

Supplemental Figure 6. Electron Micrograph of Purified PSI-LHCII Particles.

Supplemental Figure 7. Fluorescence Emission Spectra at 77K of Thylakoids Purified from *Arabidopsis* and Maize Plants in States I and II.

Supplemental Figure 8. Analysis of the Dephosphorylation of LHCII Using CIP Phosphatase.

ACKNOWLEDGMENTS

We thank Emilie Wientjes (University of Groningen) for the EM analysis and Herbert van Amerongen (University of Wageningen), Emilie Wientjes, and Roberta Croce (University of Groningen) for helpful discussion. We thank Bert Poolman (University of Groningen) and the Architecture et Fonction des Macromolécules Biologiques laboratory (Université Aix-Marseille/Centre National de la Recherche Scientifique) for the use of the spectropolarimeters. P.G. acknowledges support from the Partenariats Hubert Curien (Van Gogh). T.T.H.K. acknowledges support from the 322 project of the Vietnamese Government.

AUTHOR CONTRIBUTIONS

S.C. designed the research. S.C., P.G., S.S., T.T.H.K., and H.D. performed research. S.C., S.S., and P.G. analyzed data. S.C. and S.S. wrote the article. R.C.J., E.J.B., and P.M. contributed analytic tools and helped with article revision.

Received May 9, 2012; revised June 20, 2012; accepted July 2, 2012; published July 20, 2012.

REFERENCES

Allen, J.F. (1992). Protein phosphorylation in regulation of photosynthesis. Biochim. Biophys. Acta **1098:** 275–335.

Allen, J.F., Bennett, J., Steinback, K.E., and Arntzen, C.J. (1981). Chloroplast protein phosphorylation couples plastoquinone redox state to distribution of excitation energy between photosystems. Nature **291:** 25–29.

Amunts, A., Drory, O., and Nelson, N. (2007). The structure of a plant photosystem I supercomplex at 3.4 A resolution. Nature **447:** 58–63.

Amunts, A., Toporik, H., Borovikova, A., and Nelson, N. (2010). Structure determination and improved model of plant photosystem I. J. Biol. Chem. **285:** 3478–3486.

Bassi, R., and Dainese, P. (1992). A supramolecular light-harvesting complex from chloroplast photosystem-II membranes. Eur. J. Biochem. **204:** 317–326.

Bassi, R., Rigoni, F., Barbato, R., and Giacometti, G.M. (1988). Light-harvesting chlorophyll a/b proteins (LHCII) populations in phosphorylated membranes. Biochim. Biophys. Acta **936:** 29–38.

Bellafiore, S., Barneche, F., Peltier, G., and Rochaix, J.D. (2005). State transitions and light adaptation require chloroplast thylakoid protein kinase STN7. Nature **433:** 892–895.

Bennett, J., Steinback, K.E., and Arntzen, C.J. (1980). Chloroplast phosphoproteins: Regulation of excitation energy transfer by phosphorylation of thylakoid membrane polypeptides. Proc. Natl. Acad. Sci. USA **77:** 5253–5257.

Boekema, E.J., van Roon, H., Calkoen, F., Bassi, R., and Dekker, J.P. (1999a). Multiple types of association of photosystem II and its light-harvesting antenna in partially solubilized photosystem II membranes. Biochemistry **38:** 2233–2239.

Boekema, E.J., Van Roon, H., Van Breemen, J.F., and Dekker, J.P. (1999b). Supramolecular organization of photosystem II and its light-harvesting antenna in partially solubilized photosystem II membranes. Eur. J. Biochem. **266:** 444–452.

Bowman, J.L., Floyd, S.K., and Sakakibara, K. (2007). Green genes-comparative genomics of the green branch of life. Cell **129:** 229–234.

Broess, K., Trinkunas, G., van Hoek, A., Croce, R., and van Amerongen, H. (2008). Determination of the excitation migration time in Photosystem

II consequences for the membrane organization and charge separation parameters. Biochim. Biophys. Acta **1777:** 404–409.

Butler, W.L. (1978). Energy distribution in the photochemical apparatus of photosynthesis. Annu. Rev. Plant Physiol. **29:** 345–378.

Byrdin, M., Rimke, I., Schlodder, E., Stehlik, D., and Roelofs, T.A. (2000). Decay kinetics and quantum yields of fluorescence in photosystem I from *Synechococcus elongatus* with P700 in the reduced and oxidized state: Are the kinetics of excited state decay trap-limited or transfer-limited? Biophys. J. **79:** 992–1007.

Caffarri, S., Broess, K., Croce, R., and van Amerongen, H. (2011). Excitation energy transfer and trapping in higher plant Photosystem II complexes with different antenna sizes. Biophys. J. **100:** 2094–2103.

Caffarri, S., Croce, R., Cattivelli, L., and Bassi, R. (2004). A look within LHCII: Differential analysis of the Lhcb1-3 complexes building the major trimeric antenna complex of higher-plant photosynthesis. Biochemistry **43:** 9467–9476.

Caffarri, S., Kouril, R., Kereïche, S., Boekema, E.J., and Croce, R. (2009). Functional architecture of higher plant photosystem II supercomplexes. EMBO J. **28:** 3052–3063.

Campoli, C., Caffarri, S., Svensson, J.T., Bassi, R., Stanca, A.M., Cattivelli, L., and Crosatti, C. (2009). Parallel pigment and transcriptomic analysis of four barley albina and xantha mutants reveals the complex network of the chloroplast-dependent metabolism. Plant Mol. Biol. **71:** 173–191.

Croce, R., Canino, G., Ros, F., and Bassi, R. (2002). Chromophore organization in the higher-plant photosystem II antenna protein CP26. Biochemistry **41:** 7334–7343.

Croce, R., Dorra, D., Holzwarth, A.R., and Jennings, R.C. (2000). Fluorescence decay and spectral evolution in intact photosystem I of higher plants. Biochemistry **39:** 6341–6348.

Damkjaer, J.T., Kereïche, S., Johnson, M.P., Kovacs, L., Kiss, A.Z., Boekema, E.J., Ruban, A.V., Horton, P., and Jansson, S. (2009). The photosystem II light-harvesting protein Lhcb3 affects the macrostructure of photosystem II and the rate of state transitions in *Arabidopsis*. Plant Cell **21:** 3245–3256.

Dekker, J.P., and Boekema, E.J. (2005). Supramolecular organization of thylakoid membrane proteins in green plants. Biochim. Biophys. Acta **1706:** 12–39.

De Luca, C., Varotto, C., Svendsen, I., Polverino De Laureto, P., and Bassi, R. (1999). Multiple light-harvesting II polypeptides from maize mesophyll chloroplasts are distinct gene products. J. Photochem. Photobiol. B **49:** 50–60.

Dietzel, L., Bräutigam, K., Steiner, S., Schüffler, K., Lepetit, B., Grimm, B., Schöttler, M.A., and Pfannschmidt, T. (2011). Photosystem II supercomplex remodeling serves as an entry mechanism for state transitions in *Arabidopsis*. Plant Cell **23:** 2964–2977.

Engelmann, E., Zucchelli, G., Casazza, A.P., Brogioli, D., Garlaschi, F.M., and Jennings, R.C. (2006). Influence of the photosystem I-light harvesting complex I antenna domains on fluorescence decay. Biochemistry **45:** 6947–6955.

Engelmann, E.C.M., Zucchelli, G., Garlaschi, F.M., Casazza, A.P., and Jennings, R.C. (2005). The effect of outer antenna complexes on the photochemical trapping rate in barley thylakoid Photosystem II. Biochim. Biophys. Acta **1706:** 276–286.

Frenkel, M., Bellafiore, S., Rochaix, J.D., and Jansson, S. (2007). Hierarchy amongst photosynthetic acclimation responses for plant fitness. Physiol. Plant. **129:** 455–459.

Frigerio, S., Campoli, C., Zorzan, S., Fantoni, L.I., Crosatti, C., Drepper, F., Haehnel, W., Cattivelli, L., Morosinotto, T., and Bassi, R. (2007). Photosynthetic antenna size in higher plants is controlled by the plastoquinone redox state at the post-transcriptional rather than transcriptional level. J. Biol. Chem. **282:** 29457–29469.

Garab, G., and van Amerongen, H. (2009). Linear dichroism and circular dichroism in photosynthesis research. Photosynth. Res. **101:** 135–146.

García-Cerdán, J.G., Kovács, L., Tóth, T., Kereïche, S., Aseeva, E., Boekema, E.J., Mamedov, F., Funk, C., and Schröder, W.P. (2011). The PsbW protein stabilizes the supramolecular organization of photosystem II in higher plants. Plant J. **65:** 368–381.

Georgakopoulou, S., van der Zwan, G., Bassi, R., van Grondelle, R., van Amerongen, H., and Croce, R. (2007). Understanding the changes in the circular dichroism of light harvesting complex II upon varying its pigment composition and organization. Biochemistry **46:** 4745–4754.

Gobets, B., Kennis, J.T.M., Ihalainen, J.A., Brazzoli, M., Croce, R., van Stokkum, I.H.M., Bassi, R., Dekker, J.P., Van Amerongen, H., Fleming, G.R., and van Grondelle, R. (2001). Excitation energy transfer in dimeric light harvesting complex I: A combined streak-camera/fluorescence upconversion study. J. Phys. Chem. B **105:** 10132–10139.

Hankamer, B., Nield, J., Zheleva, D., Boekema, E., Jansson, S., and Barber, J. (1997). Isolation and biochemical characterisation of monomeric and dimeric photosystem II complexes from spinach and their relevance to the organisation of photosystem II in vivo. Eur. J. Biochem. **243:** 422–429.

Ihalainen, J.A., van Stokkum, I.H.M., Gibasiewicz, K., Germano, M., van Grondelle, R., and Dekker, J.P. (2005). Kinetics of excitation trapping in intact Photosystem I of *Chlamydomonas reinhardtii* and *Arabidopsis thaliana*. Biochim. Biophys. Acta **1706:** 267–275.

Iwai, M., Takahashi, Y., and Minagawa, J. (2008). Molecular remodeling of photosystem II during state transitions in *Chlamydomonas reinhardtii*. Plant Cell **20:** 2177–2189.

Jansson, S. (1999). A guide to the Lhc genes and their relatives in *Arabidopsis*. Trends Plant Sci. **4:** 236–240.

Järvi, S., Suorsa, M., Paakkarinen, V., and Aro, E.M. (2011). Optimized native gel systems for separation of thylakoid protein complexes: Novel super- and mega-complexes. Biochem. J. **439:** 207–214.

Jennings, R.C., Zucchelli, G., Croce, R., and Garlaschi, F.M. (2003). The photochemical trapping rate from red spectral states in PSI-LHCI is determined by thermal activation of energy transfer to bulk chlorophylls. Biochim. Biophys. Acta **1557:** 91–98.

Jensen, P.E., Bassi, R., Boekema, E.J., Dekker, J.P., Jansson, S., Leister, D., Robinson, C., and Scheller, H.V. (2007). Structure, function and regulation of plant photosystem I. Biochim. Biophys. Acta **1767:** 335–352.

Jensen, P.E., Haldrup, A., Zhang, S.P., and Scheller, H.V. (2004). The PSI-O subunit of plant photosystem I is involved in balancing the excitation pressure between the two photosystems. J. Biol. Chem. **279:** 24212–24217.

Kargul, J., Turkina, M.V., Nield, J., Benson, S., Vener, A.V., and Barber, J. (2005). Light-harvesting complex II protein CP29 binds to photosystem I of *Chlamydomonas reinhardtii* under State 2 conditions. FEBS J. **272:** 4797–4806.

Kouril, R., Zygadlo, A., Arteni, A.A., de Wit, C.D., Dekker, J.P., Jensen, P.E., Scheller, H.V., and Boekema, E.J. (2005). Structural characterization of a complex of photosystem I and light-harvesting complex II of *Arabidopsis thaliana*. Biochemistry **44:** 10935–10940.

Laemmli, U.K. (1970). Cleavage of structural proteins during the assembly of the head of bacteriophage T4. Nature **227:** 680–685.

Lemeille, S., and Rochaix, J.D. (2010). State transitions at the crossroad of thylakoid signalling pathways. Photosynth. Res. **106:** 33–46.

Lemeille, S., Willig, A., Depège-Fargeix, N., Delessert, C., Bassi, R., and Rochaix, J.D. (2009). Analysis of the chloroplast protein kinase Stt7 during state transitions. PLoS Biol. **7:** e45.

Liu, Z., Yan, H., Wang, K., Kuang, T., Zhang, J., Gui, L., An, X., and Chang, W. (2004). Crystal structure of spinach major light-harvesting complex at 2.72 A resolution. Nature **428:** 287–292.

Lunde, C., Jensen, P.E., Haldrup, A., Knoetzel, J., and Scheller, H.V. (2000). The PSI-H subunit of photosystem I is essential for state transitions in plant photosynthesis. Nature **408:** 613–615.

Mctavish, H. (1988). A demonstration of photosynthetic state transitions in nature - Shading by photosynthetic tissue causes conversion to state-1. Photosynth. Res. **17:** 247–254.

Minagawa, J. (2011). State transitions—The molecular remodeling of photosynthetic supercomplexes that controls energy flow in the chloroplast. Biochim. Biophys. Acta **1807:** 897–905.

Morosinotto, T., Bassi, R., Frigerio, S., Finazzi, G., Morris, E., and Barber, J. (2006). Biochemical and structural analyses of a higher plant photosystem II supercomplex of a photosystem I-less mutant of barley. Consequences of a chronic over-reduction of the plastoquinone pool. FEBS J. **273:** 4616–4630.

Moya, I., Silvestri, M., Vallon, O., Cinque, G., and Bassi, R. (2001). Time-resolved fluorescence analysis of the photosystem II antenna proteins in detergent micelles and liposomes. Biochemistry **40:** 12552–12561.

Oostergetel, G.T., Keegstra, W., and Brisson, A. (1998). Automation of specimen selection and data acquisition for protein electron crystallography. Ultramicroscopy **74:** 47–59.

Peter, G.F., and Thornber, J.P. (1991). Biochemical composition and organization of higher plant photosystem II light-harvesting pigment-proteins. J. Biol. Chem. **266:** 16745–16754.

Pribil, M., Pesaresi, P., Hertle, A., Barbato, R., and Leister, D. (2010). Role of plastid protein phosphatase TAP38 in LHCII dephosphorylation and thylakoid electron flow. PLoS Biol. **8:** e1000288.

Qin, X., Wang, W., Wang, K., Xin, Y., and Kuang, T. (2011). Isolation and characteristics of the PSI-LHCI-LHCII supercomplex under high light. Photochem. Photobiol. **87:** 143–150.

Remelli, R., Varotto, C., Sandonà, D., Croce, R., and Bassi, R. (1999). Chlorophyll binding to monomeric light-harvesting complex. A mutation analysis of chromophore-binding residues. J. Biol. Chem. **274:** 33510–33521.

Rintamäki, E., Martinsuo, P., Pursiheimo, S., and Aro, E.M. (2000). Cooperative regulation of light-harvesting complex II phosphorylation via the plastoquinol and ferredoxin-thioredoxin system in chloroplasts. Proc. Natl. Acad. Sci. USA **97:** 11644–11649.

Ruban, A.V., and Johnson, M.P. (2009). Dynamics of higher plant photosystem cross-section associated with state transitions. Photosynth. Res. **99:** 173–183.

Shapiguzov, A., Ingelsson, B., Samol, I., Andres, C., Kessler, F., Rochaix, J.D., Vener, A.V., and Goldschmidt-Clermont, M. (2010). The PPH1 phosphatase is specifically involved in LHCII dephosphorylation and state transitions in *Arabidopsis*. Proc. Natl. Acad. Sci. USA **107:** 4782–4787.

Szopinska, A., Degand, H., Hochstenbach, J.F., Nader, J., and Morsomme, P. (2011). Rapid response of the yeast plasma membrane proteome to salt stress. Mol. Cell. Proteomics **10:** M111.009589.

Takahashi, H., Iwai, M., Takahashi, Y., and Minagawa, J. (2006). Identification of the mobile light-harvesting complex II polypeptides for state transitions in *Chlamydomonas reinhardtii*. Proc. Natl. Acad. Sci. USA **103:** 477–482.

Tikkanen, M., Grieco, M., Kangasjärvi, S., and Aro, E.M. (2010). Thylakoid protein phosphorylation in higher plant chloroplasts optimizes electron transfer under fluctuating light. Plant Physiol. **152:** 723–735.

Tikkanen, M., Nurmi, M., Suorsa, M., Danielsson, R., Mamedov, F., Styring, S., and Aro, E.M. (2008). Phosphorylation-dependent regulation of excitation energy distribution between the two photosystems in higher plants. Biochim. Biophys. Acta **1777:** 425–432.

Tikkanen, M., Piippo, M., Suorsa, M., Sirpiö, S., Mulo, P., Vainonen, J., Vener, A.V., Allahverdiyeva, Y., and Aro, E.M. (2006). State transitions revisited-a buffering system for dynamic low light acclimation of *Arabidopsis*. Plant Mol. Biol. **62:** 779–793. Erratum Plant Mol. Biol. **62:** 795.

Tumino, G., Casazza, A.P., Engelmann, E., Garlaschi, F.M., Zucchelli, G., and Jennings, R.C. (2008). Fluorescence lifetime spectrum of the plant photosystem II core complex: Photochemistry does not induce specific reaction center quenching. Biochemistry **47:** 10449–10457.

Turconi, S., Kruip, J., Schweitzer, G., Rogner, M., and Holzwarth, A.R. (1996). A comparative fluorescence kinetics study of photosystem I monomers and trimers from Synechocystis PCC 6803. Photosynth. Res. **49:** 263–268.

van Oort, B., Alberts, M., de Bianchi, S., Dall'Osto, L., Bassi, R., Trinkunas, G., Croce, R., and van Amerongen, H. (2010). Effect of antenna-depletion in Photosystem II on excitation energy transfer in *Arabidopsis thaliana*. Biophys. J. **98:** 922–931.

van Oort, B., Amunts, A., Borst, J.W., van Hoek, A., Nelson, N., van Amerongen, H., and Croce, R. (2008). Picosecond fluorescence of intact and dissolved PSI-LHCI crystals. Biophys. J. **95:** 5851–5861.

Wagner, R., Dietzel, L., Bräutigam, K., Fischer, W., and Pfannschmidt, T. (2008). The long-term response to fluctuating light quality is an important and distinct light acclimation mechanism that supports survival of *Arabidopsis thaliana* under low light conditions. Planta **228:** 573–587.

Wientjes, E., and Croce, R. (2011). The light-harvesting complexes of higher-plant Photosystem I: Lhca1/4 and Lhca2/3 form two red-emitting heterodimers. Biochem. J. **433:** 477–485.

Wientjes, E., van Stokkum, I.H., van Amerongen, H., and Croce, R. (2011). Excitation-energy transfer dynamics of higher plant photosystem I light-harvesting complexes. Biophys. J. **100:** 1372–1380.

Williams, W.P., and Allen, J.F. (1987). State-1/State-2 changes in higher-plants and algae. Photosynth. Res. **13:** 19–45.

Wollman, F.A. (2001). State transitions reveal the dynamics and flexibility of the photosynthetic apparatus. EMBO J. **20:** 3623–3630.

Zhang, S., and Scheller, H.V. (2004). Light-harvesting complex II binds to several small subunits of photosystem I. J. Biol. Chem. **279:** 3180–3187.

Zuker, M., Szabo, A.G., Bramall, L., Krajcarski, D.T., and Selinger, B.K. (1985). Delta-function convolution method (DFCM) for fluorescence decay experiments. Rev. Sci. Instrum. **56:** 14–22.